Oncology Research, Vol. 26, pp. 519–528
Printed in the USA.

0965-0407/18 $90.00 + .00
DOI: https://doi.org/10.3727/096504017X15000757094686
E-ISSN 1555-3906
www.cognizantcommunication.com

miR-103 Functions as a Tumor Suppressor by Directly Targeting Programmed Cell Death 10 in NSCLC

Dong Yang, Jian-Jun Wang, Jin-Song Li, and Qian-Yu Xu

Department of Thoracic Surgery, Union Hospital, Tongji Medical College,
Huazhong University of Science and Technology, Wuhan, Hubei, P.R. China

Non-small cell lung cancer (NSCLC) accounts for about 85% of all lung cancer cases. Absence of miR-103 has recently been identified to be associated with metastatic capacity of primary lung tumors. However, the exact role of miR-103 in NSCLC and the molecular mechanism are unclear. In the present study, we showed that miR-103 expression was reduced in NSCLC tissues and cells. miR-103 expression was negatively correlated with tumor size and stage. The overall survival was longer in patients with higher miR-103 level than in those with lower miR-103 expression. miR-103 inhibited cell proliferation in A549 cells, decreased tumor weight and volume, and prolonged survival of tumor-implanted nude mice. miR-103 increased apoptotic cell death in A549 cells. Furthermore, miR-103 decreased the invasion and migration abilities in A549 cells, as evidenced by Transwell and wound healing results. Downregulation of miR-103 significantly reduced the level of programmed cell death 10 (PDCD10). We found a significant decrease in the relative luciferase activity of the reporter gene in A549 cells cotransfected with the miR-103 mimic and pGL3-PDCD10 WT 3′-UTR, but not pGL3-PDCD10 mut 3′-UTR. We showed that overexpression of PDCD10 significantly inhibited miR-103-induced inhibition of cell proliferation, increased apoptosis, and decreased invasion and migration in A549 cells. Moreover, we found that PDCD10 expression was increased in NSCLC tissues and cells. PDCD10 expression was positively correlated with tumor size and stage. Overexpression of PDCD10 increased cell proliferation and inhibited apoptosis in A549 cells. The data demonstrated that dysregulation of the miR-103/PDCD10 signal may be a novel therapeutic target for the treatment of NSCLC.

Key words: MicroRNA-103 (miR-103); Programmed cell death 10 (PDCD10); Non-small cell lung cancer (NSCLC); Proliferation; Apoptosis

INTRODUCTION

Lung cancer is a type of common and deadly cancer among both men and women. In China, lung cancer has become the most common human carcinoma, with the highest cancer-related mortality rate among both men and women, which may be attributed to loose regulation and deteriorating air quality[1,2]. There are two major subtypes of human lung carcinoma, non-small cell lung cancer (NSCLC) and small lung cancer (SCLC). NSCLC accounts for about 85% of all lung cancer cases, which also include adenocarcinoma, large cell carcinoma, and squamous cell carcinoma[3,4]. Nowadays, therapies for NSCLC are surgery combined with chemotherapy and radiotherapy. The therapeutic strategy can be applied according to the range and progression of the disease[5]. Five-year survival rates can reach 20%–30% in NSCLC patients after surgery[6]. However, local and distant metastasis is a common clinical problem during the treatment of lung cancer and is the primary contributor to poor prognosis in many patients[7]. Therefore, early diagnosis is critical for the therapy of NSCLC patients. Exploration of novel molecular targets and biomarkers may improve NSCLC therapy.

MicroRNAs (miRNAs) are a class of noncoding single-stranded RNAs approximately 18–22 nucleotides in length that play important roles in the regulation of cell differentiation, proliferation, apoptosis, and metabolism[8]. miRNAs bind to the complimentary DNA sequence on the 3′-untranslated region (3′-UTR) of targeted genes and posttranscriptionally inhibit target gene expression, modulating multiple biological processes[9,10]. It has been verified that regulation of miRNAs is involved in the critical stages of carcinoma development, such as tumorigenesis, tumor metastasis, or apoptosis[11]. Abnormal expression of a battery of miRNAs is involved in the development of NSCLC[12,13]. miR-103 plays both an

Address correspondence to Jian-Jun Wang, Department of Thoracic Surgery, Union Hospital, Tongji Medical College,
Huazhong University of Science and Technology, 1277 Jiefang Road, Wuhan, Hubei 430022, P.R. China. E-mail: wangjianjununione@126.com

oncogenic and tumor-suppressive role in various types of cancers. miR-103 promotes colorectal cancer by targeting tumor suppressors DICER and PTEN[14]. miR-103 inhibits proliferation and sensitizes hemopoietic tumor cells for glucocorticoid-induced apoptosis[15]. miR-103 regulates migration and invasion of triple negative breast cancer cells through targeting olfactomedin 4[16]. A recent study showed that the absence of miR-103 can be used to identify primary lung tumors with metastatic capacity[17]. However, the exact role of miR-103 in NSCLC and the molecular mechanism are unclear.

In the present study, we report that miR-103 was upregulated and programmed cell death 10 (PDCD10) was downregulated in NSCLC tissues and cell lines. Low expression of miR-103 was associated with worse patient prognosis. miR-103 inhibited NSCLC cell proliferation, induced apoptotic cell death, and inhibited migration. Overexpression of PDCD10 suppressed miR-103-induced inhibitory effect on NSCLC cell proliferation and migration. Moreover, miR-103 decreased tumor volume and weight in implanted tumors, decreased the survival of animals, and reduced PDCD10 expression in transplanted tumors. The results demonstrated that miR-103 acted as a tumor suppressor through targeting PDCD10 in NSCLC.

MATERIALS AND METHODS

Patients, Tissues, and Ethics Statement

The study protocol was approved by the ethics committee of Union Hospital, Tongji Medical College, Huazhong University of Science and Technology. A total of 32 fresh primary NSCLC tissues and matched adjacent noncancerous lung tissues were collected at the Department of Thoracic Surgery, Union Hospital, Tongji Medical College, Huazhong University of Science and Technology. The diagnosis of all specimens was histopathologically confirmed by two pathologists according to the WHO criteria for lung cancer. The tissues samples were obtained from patients who did not receive chemoradiotherapy. For living patients, overall survival was defined as the amount of time from the day of primary surgery to the date of death or the end of follow-up. All the patients signed informed consent forms.

Cell Culture and Transfection

NSCLS cell lines (A549, SPC-A1, NCI-H460, H1299, and PC9), the HEK-293T cell line, and the normal human bronchial epithelial cell line (16HBE) were all obtained from the Institute of Biochemistry and Cell Biology of the Chinese Academy of Sciences (Shanghai, P.R. China). The cells were routinely cultured in Dulbecco's modified Eagle's medium (Gibco, Grand Island, NY, USA) supplemented with 10% fetal bovine serum (FBS; Gibco, Thermo Fisher Scientific, Waltham, MA, USA), 100 U/ml penicillin, and 100 μg/ml streptomycin and incubated at 37°C and 5% CO_2. A549 cells were transiently transfected with the miR-103 mimic, negative control mimic (NC), miR-103 inhibitor, pcDNA 3.1 PDCD10, or negative control siRNA (pcDNA 3.1) using Invitrogen™ Lipofectamine 2000 (Life Technologies, Grand Island, NY, USA) according to the manufacturer's recommendations. At 24–48 h after the transfections, cells were used for subsequent experiments.

Cell Proliferation

Cell proliferation was measured by the cell counting kit-8 (CCK-8) assay kit (Beyotime Biotechnology, Jiangsu, P.R. China). At 24, 48, and 72 h after the culture, 8 μl of CCK-8 solution and 100 μl of serum-free medium were added to each well and then incubated for 90 min. Finally, the absorbance was measured at 450 nm using a microplate reader. Each data point represented the measurement of three replicate wells.

Apoptosis Analysis

Apoptosis was detected by TUNEL staining using the In Situ Cell Death Detection Kit, Fluorescein (Roche, Basel, Switzerland) following the manufacturer's instructions. The percentage of apoptotic cells was analyzed by flow cytometry (BD Biosciences, San Jose, CA, USA).

Quantitative Real-Time PCR

Total RNA was isolated using TRIzol reagent (Invitrogen, Carlsbad, CA, USA) according to the manufacturer's protocol. cDNA synthesis was performed with the SYBR PrimeScript miRNA RT-PCR Kit and PrimeScript RT Master Mix (Takara Biotech, Otsu, Japan) following the manufacturer's instructions. miRNA and mRNA were measured by qRT-PCR using SYBR Green II (Takara Biotech) performed according to the manufacturer's protocol on a CFX96™ Real-Time System (Bio-Rad, Hercules, CA, USA). miR-103 was quantified by normalization to U6 expression level, and PDCD10 was quantified by normalization to β-actin level. The expression levels of miRNAs and mRNAs were determined by the $2^{-\Delta\Delta}$Ct method for relative quantification of gene expression.

Western Blot Analysis

Cells and tissues were lysed using radioimmunoprecipitation assay (RIPA) lysis buffer (CWBIO, Beijing, P.R. China). The protein concentration was quantified by a Bradford protein assay (Thermo Fisher Scientific). Equal amounts of protein from each sample were separated on 10% denaturing polyacrylamide gels (with 5% polyacrylamide stacking gel) and transferred electrophoretically onto a polyvinylidene fluoride membrane (Millipore Corporation, Billerica, MA, USA). The membrane

was then soaked in Tris-buffered saline with Tween 20 [TBST; 150 mM NaCl, 20 mM Tris-HCl (pH 8.0), 0.05% Tween 20] containing 55% nonfat dry milk for 1 h at room temperature. Then the membranes were incubated with primary antibodies at 4°C overnight. Afterward, the membranes were incubated with HRP-conjugated secondary antibody (Thermo Fisher Scientific). Protein bands were detected by chemiluminescence reaction using an enhanced chemiluminescence detection system (Millipore Corporation), captured using Bio-Rad Imaging Systems, and analyzed by Image Lab analysis software (Bio-Rad).

Dual-Luciferase Reporter Assay

The PDCD10 wild-type (WT) 3′-UTR firefly luciferase construct (pGL3-PDCD10 WT 3′-UTR) and the pGL3-PDCD10 mutant (mut) 3′-UTR construct were generated. A549 cells were cotransfected with 100 ng of pGL3-PDCD10 WT 3′-UTR or pGL3-PDCD10 mut 3′-UTR luciferase reporter and 15 ng of *Renilla* luciferase reporter (pRL), and a final concentration of 100 nM miRNA NC or miR-103 mimic using Invitrogen™ Lipofectamine 2000 (Life Technologies). Forty-eight hours after the incubation, cells were washed with cold PBS, lysed in 200 µl of lysis buffer, and then centrifuged at 12,000 rpm for 2 min at 4°C. The supernatants were used for the detection of luciferase activity using a dual-luciferase reporter assay system (Promega, Beijing, P.R. China). Firefly luciferase units were normalized against *Renilla* luciferase units to control for transfection efficiency. Relative activities were expressed as the fold change in luciferase activity.

Migration Assays

The cell invasion ability was evaluated by Transwell assay using Matrigel-coated cell culture chambers (8-µm pore size; EMD Millipore). Cells (1×10^5) were added to the upper chamber with 100 µl of serum-free medium, and 600 µl of medium with 10% FBS was added to the lower chamber. The cells were cultured for 24 h at 37°C. The cells remaining on the upper membrane were carefully removed. Cells on the lower membrane were fixed and stained with crystal violet. The cell population was calculated using a light microscope (Nikon, Tokyo, Japan) and was expressed as the fold change of control.

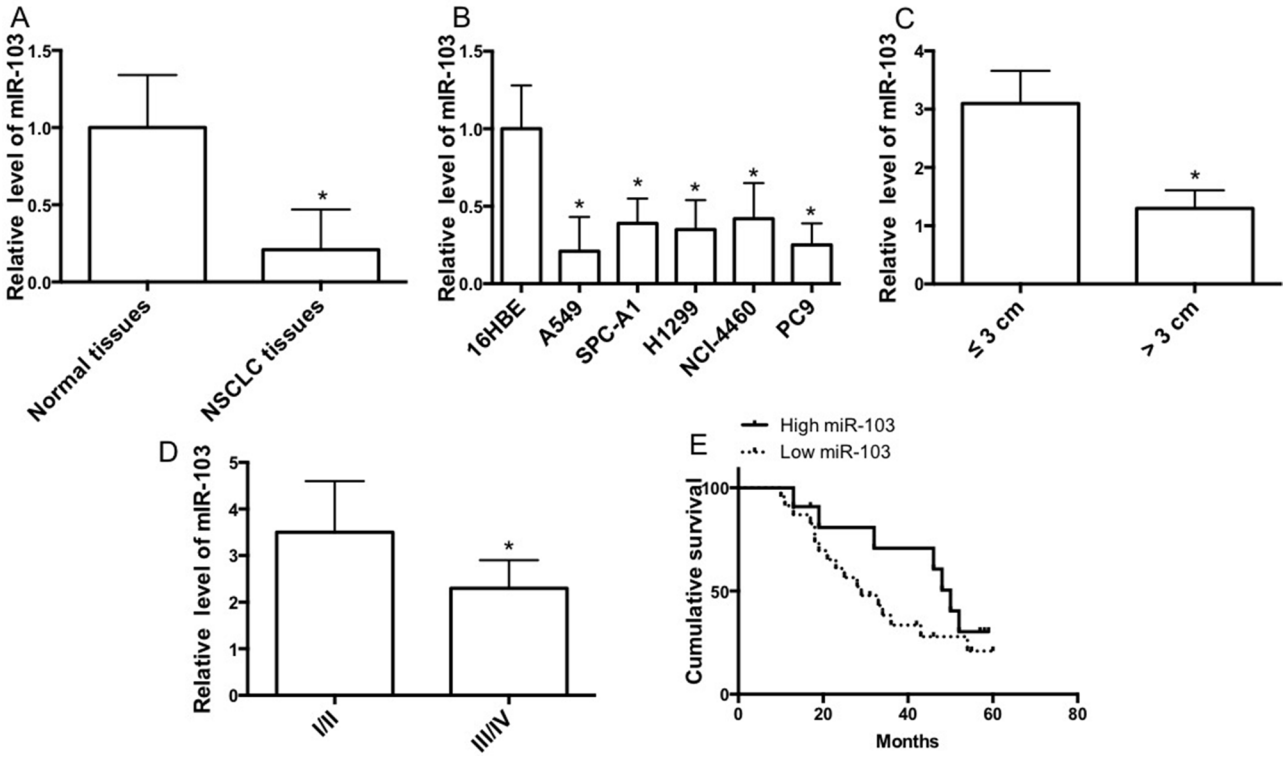

Figure 1. miR-103 is upregulated in non-small cell lung cancer (NSCLC) tissues and cell lines. (A) The relative mRNA expression level of miR-103 in tumor tissues and corresponding nontumor tissues. (B) The relative mRNA expression level of miR-103 in lung cancer cell lines and 16HBE cells was measured by quantitative real-time (qRT)-PCR ($n=3$ independent experiments). (C) Expression of miR-103 related to tumor size. (D) Expression of miR-103 related to tumor pathological stage. (E) Kaplan–Meier analyses of cumulative survival for patients with NSCLC according to the expression of miR-103. Error bars represent the mean ± SEM. *$p<0.05$, compared with control.

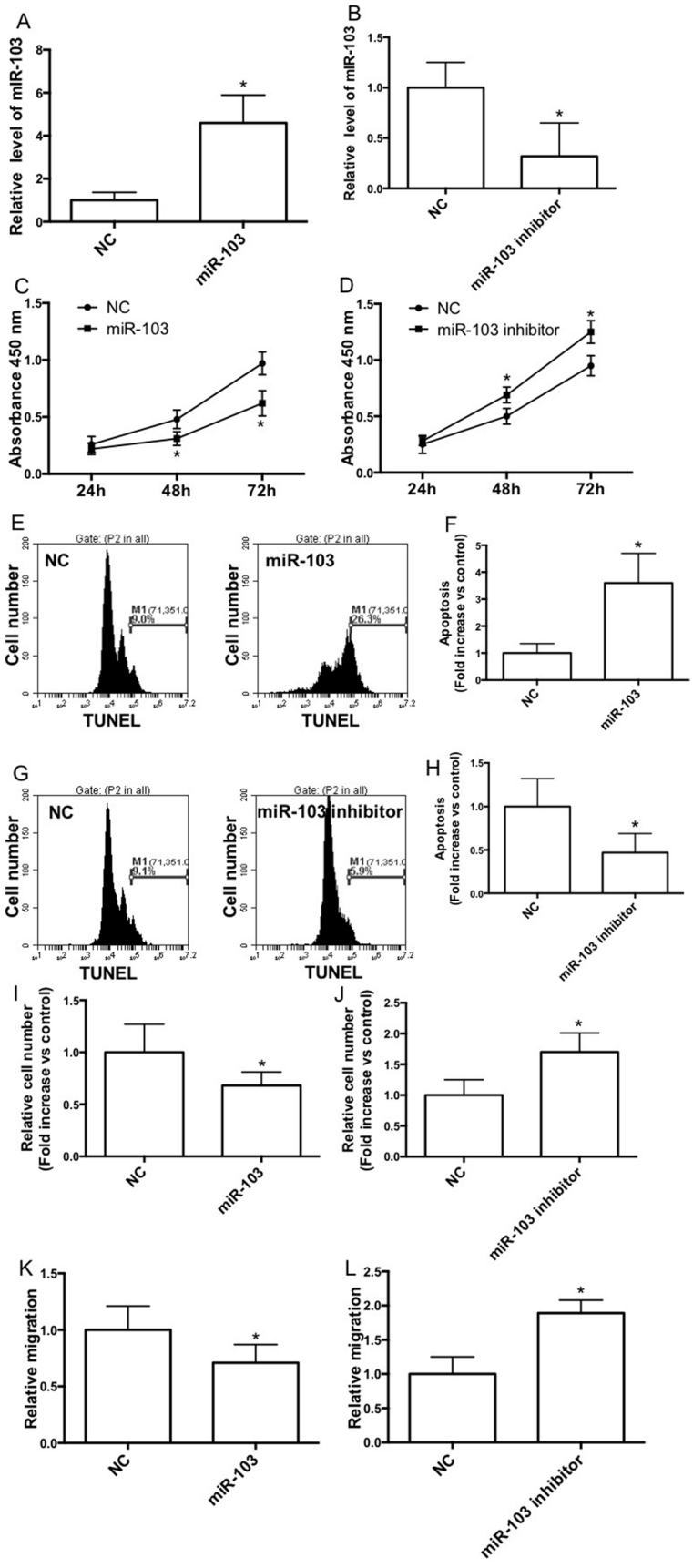
A
Relative level of miR-103
NC
miR-103
B
Relative level of miR-103
NC
miR-103 inhibitor
C
Absorbance 450 nm
NC
miR-103
24h
48h
72h
D
Absorbance 450 nm
NC
miR-103 inhibitor
24h
48h
72h
E
Gate: (P2 in all)
NC
Cell number
TUNEL
Gate: (P2 in all)
miR-103
Cell number
TUNEL
F
Apoptosis
(Fold increase vs control)
NC
miR-103
G
Gate: (P2 in all)
NC
Cell number
TUNEL
Gate: (P2 in all)
miR-103 inhibitor
Cell number
TUNEL
H
Apoptosis
(Fold increase vs control)
NC
miR-103 inhibitor
I
Relative cell number
(Fold increase vs control)
NC
miR-103
J
Relative cell number
(Fold increase vs control)
NC
miR-103 inhibitor
K
Relative migration
NC
miR-103
L
Relative migration
NC
miR-103 inhibitor

In the wound healing assay, cells were seeded in 24-well plates and cultured to 100%. A single scratch wound was made in the center of the well by a sterile pipette tip. Cell debris was removed by washing with PBS, and cells were allowed to grow in the serum-free medium. The migration distance of the cells was photographed at 24 h by a microscope (Nikon) and expressed as fold change of control.

Lentivirus Construction

pLenti-miR-103 or pLenti vector was cotransfected into HEK-293T cells with psPAX2 and pMD2G. Forty-eight and 72 h later, viral particles were collected and centrifuged together at 4,000 rpm for 5 min at 4°C and then filtered through 0.45-μm filters.

Tumor Xenograft In Vivo

All animal procedures were approved by the Ethics Animal Care and Use Committee of Tongji Medical College, Huazhong University of Science and Technology. To confirm the antitumor function of miR-103 in vivo, 1×10^7 logarithmically growing A549 cells stably transfected with lenti-miR-NC or lenti-miR-103 were suspended in a 1:1 mixture of culture medium and growth factor-reduced Matrigel and injected subcutaneously into the right armpit of male BALB/c nude mice (18–26 g). Four days after the implantation, the mice were treated with the following two protocols. In protocol 1, the mice were randomly divided into two groups, 10 mice per group. Four weeks after the inoculation, all mice were sacrificed, and the tumors were excised, weighed, and subjected to qRT-PCR and Western blot. In protocol 2, the mice were randomly divided into two groups, 20 mice per group. The survival of nude mice was observed up to 80 days.

Statistical Analysis

All data were expressed as the mean ± SEM, and statistical analyses were performed using GraphPad Prism software. The differences between the two groups were evaluated with two-sided unpaired Student's *t*-tests. The differences among more than two groups were evaluated by one-way analysis of variance (ANOVA) followed by a Dunnett's *t*-test for multiple comparisons. Survival was evaluated by the Kaplan–Meier analysis. A value of $p<0.05$ was considered to be statistically significant.

RESULTS

miR-103 Expression Is Increased in NSCLC Tissues and Cell Lines

In order to clarify the role of miR-103 in lung carcinogenesis, we detected the expression level in lung cancer tissues of NSCLC patient cases. We showed that miR-103 expression was reduced in tumor tissues compared with corresponding nontumor lung tissues (Fig. 1A). Consistent with the results, miR-103 expression was decreased in several NSCLC cell lines, compared with 16HBE cells (Fig. 1B). miR-103 expression level in tumors larger than 3 cm was lower than in tumors smaller than 3 cm (Fig. 1C). Moreover, miR-103 expression level in stage III/IV tumors was lower than in stage I/II tumors (Fig. 1D). Furthermore, Kaplan–Meier analysis was carried out to evaluate the correlation of miR-103 level with the overall survival of NSCLC patients. Survival analysis revealed that the median overall survival was longer in patients with higher miR-103 expression than in those with lower miR-103 expression (Fig. 1E). Our data demonstrated that miR-103 was negatively associated with the development of NSCLC and was a positive prognostic factor in NSCLC patients.

miR-103 Inhibits Cell Proliferation and Migration in the A549 Cell Line

To study the effect of miR-103 on NSCLC cell proliferation, A549 cells were transfected with the miR-103 mimic or inhibitor, and qRT-PCR analysis was conducted to confirm the transfection efficiency (Fig. 2A and B). The proliferation of A549 cells was examined by the CCK-8 assay (Fig. 2C and D). The results showed that transfection with the miR-103 mimic significantly inhibited the cell growth after 48 h (Fig. 2C), whereas the miR-103 inhibitor increased cell proliferation notably under the same culture conditions (Fig. 2D). Moreover, miR-103 mimic transfection significantly increased the TUNEL-stained cell population (Fig. 2E and F), indicating the increase of apoptotic cell death. The miR-103 inhibitor notably decreased the apoptosis in A549 cells (Fig. 2G and H). In the invasion test, we showed that the miR-103 mimic remarkably decreased the Transwell cell number (Fig. 2I) and the miR-103 inhibitor increased the cell number on the lower membrane (Fig. 2J). Furthermore,

FACING PAGE

Figure 2. miR-103 inhibits cell proliferation and migration of the A549 cell line. A549 cells were transfected with the negative control mimic (NC) or the miR-103 mimic/NC or the miR-103 inhibitor. miR-103 expression was determined by qRT-PCR (A, B), and cell proliferation was determined by the cell counting kit-8 (CCK-8) assay kit. (C, D). The apoptosis distributions of A549 cells transfected with NC or the miR-103 mimic/NC or the miR-103 inhibitor for 48 h, which was detected by flow cytometry (E, G) and expressed as fold increase versus control (F, H). (I–L) Forty-eight hours after the transfection with NC or the miR-103 mimic/NC or the miR-103 inhibitor, wound healing assays and Transwell assays were performed in A549 cells. $n=3$–4 independent experiments. Error bars represent the mean ± SEM. $^*p<0.05$, compared with control.

the miR-103 mimic reduced the relative migration distance (Fig. 2K), and the miR-103 inhibitor increased the distance of migration in wound healing assays (Fig. 2L).

miR-103 Directly Targets PDCD10

We selected PDCD10 as a potential target of miR-103 using the TargetScan prediction programs (www.targetscan.org) (Fig. 3A). To confirm whether PDCD10 is a direct target of miR-103, the PDCD10 WT 3′-UTR was cloned into the pGL3 vector (pGL3-PDCD10 WT 3′-UTR) downstream of the luciferase open reading frame. In order to validate target specificity, we mutated the miR-103 binding sites and conducted site-directed mutagenesis for PDCD10 WT 3′-UTR using the QuikChange Mutagenesis Kit (Fig. 3A). We found a significant decrease in the relative luciferase activity of the reporter gene in A549 cells cotransfected with pGL3-PDCD10 WT 3′-UTR and the miR-103 mimic (Fig. 3B). Conversely, cotransfection of miR-103 with pGL3-PDCD10 mut 3′-UTR resulted in no significant change in luciferase activity (Fig. 3B). Furthermore, we observed that the miR-103 mimic remarkably reduced PDCD10 mRNA and protein expression in cells (Fig. 3C and D). We detected the expression level in lung cancer tissues of NSCLC patient cases. We showed

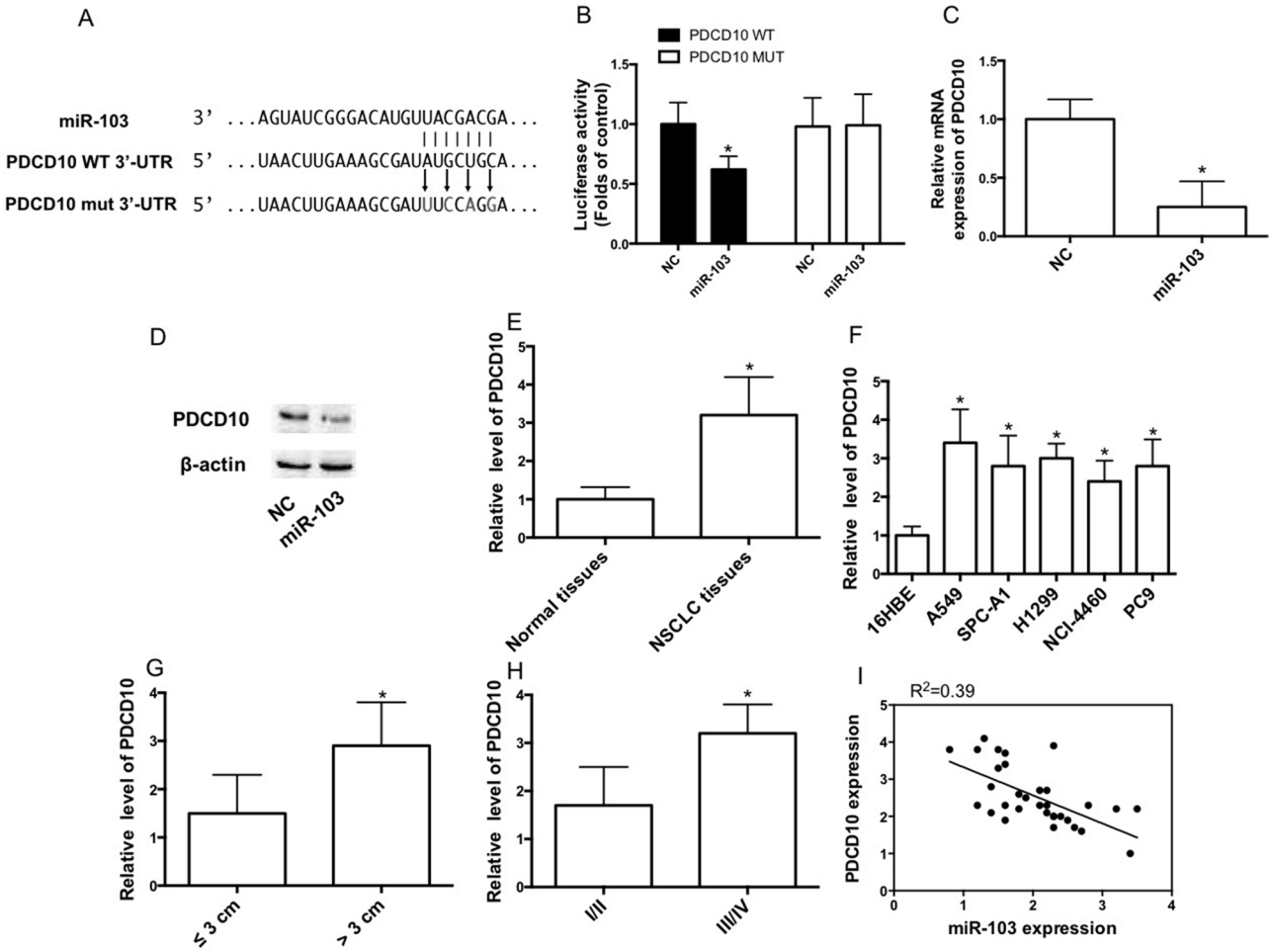

Figure 3. Programmed cell death 10 (PDCD10) is a direct target of miR-103. (A) PDCD10 wild-type (WT) 3′-untranslated region (3′-UTR) contains predicted miR-103 binding sites. Alignment of miR-103 with the PDCD10 WT 3′-UTR, with arrows indicating the mutagenesis nucleotides. (B) Dual-luciferase reporter assay. A549 cells were cotransfected with luciferase reporter constructs containing the pGL3-PDCD10 WT 3′-UTR (PDCD10 WT) and the pGL3-PDCD10 mutant (mut) 3′-UTR (PDCD10 MUT) with the miR-103 mimic or NC mimic. Relative firefly luciferase expression was normalized to *Renilla* luciferase expression. (C, D) The mRNA and protein expression of PDCD10 IN A549 cells transfected with NC or the miR-103 mimic. (E) The relative mRNA expression level of PDCD10 in tumor tissues and corresponding nontumor tissues. (F) The relative mRNA expression level of PDCD10 in lung cancer cell lines and 16HBE cells was measured by qRT-PCR. (G) Expression of PDCD10 related to tumor size. (H) Expression of PDCD10 related to tumor pathological stage. (I) miR-103 had a negative correlation with PDCD10 according to Pearson correlation coefficient. $n = 3$ independent experiments. Error bars represent the mean ± SEM. $^*p < 0.05$, compared with control.

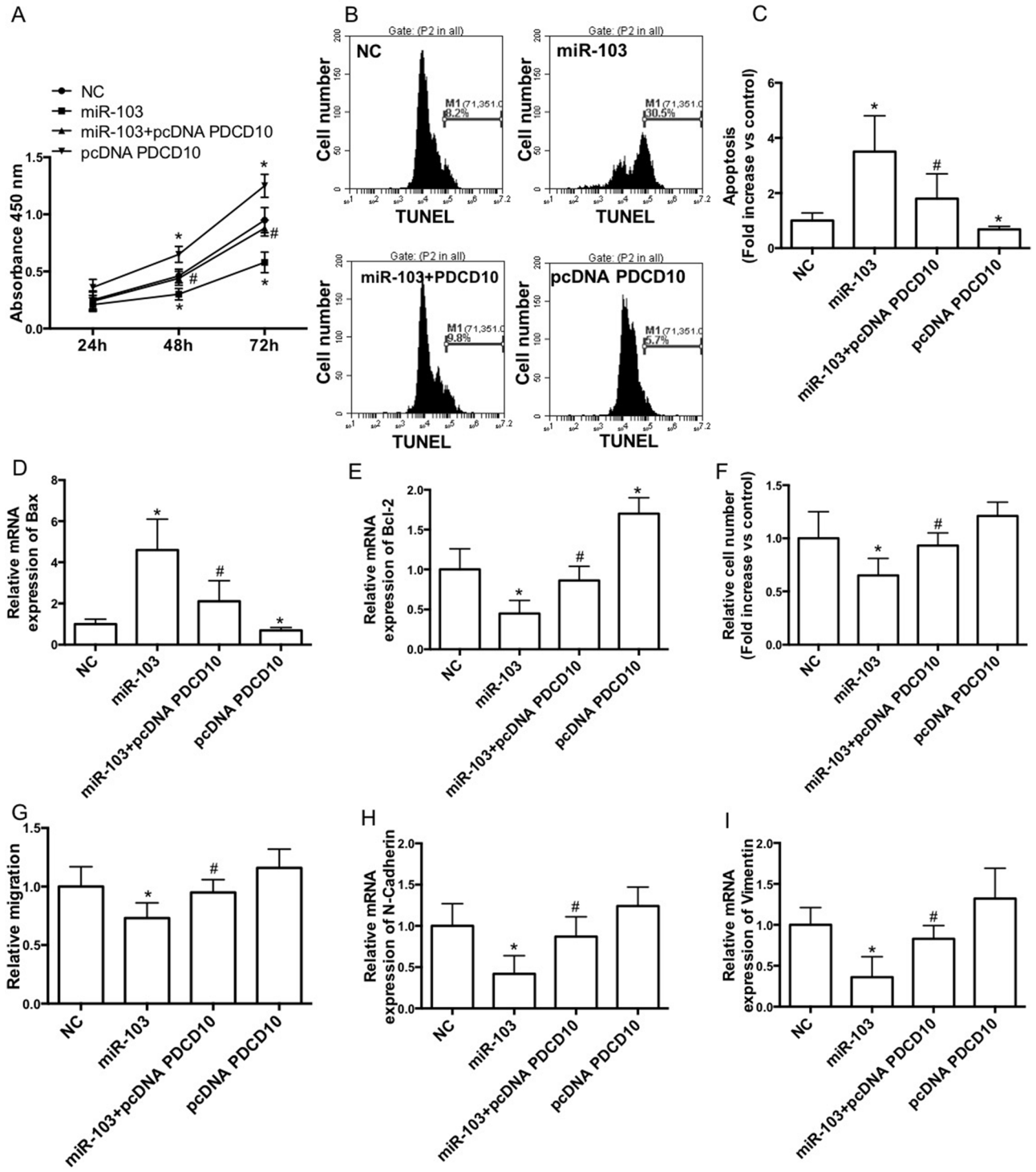

Figure 4. Downregulation of PDCD10 is involved in miR-103-induced inhibition of proliferation and migration of A549 cell line. A549 cells were cotransfected with NC or the miR-103 mimic and pcDNA or pcDNA PDCD10. (A) Cell proliferation was determined by the CCK-8 assay kit. (B, C) The apoptosis distribution was detected by flow cytometry (B) and expressed as fold increase versus control (C). mRNA expression of Bax (D) and Bcl-2 (E) was determined by qRT-PCR and expressed as folds of control. Transwell assays (F) and wound healing assays (G) were performed in A549 cells. mRNA expression of Bax (H) and Bcl-2 (I) was determined by qRT-PCR and expressed as fold of control. $n = 3$–4 independent experiments. Error bars represent the mean ± SEM. *$p < 0.05$, compared with control. #$p < 0.05$, compared with miR-103.

that PDCD10 expression was increased in tumor tissues, compared with corresponding nontumor lung tissues (Fig. 3E). Consistent with the results, PDCD10 expression was increased in several NSCLC cell lines, compared with 16HBE cells (Fig. 3F). The PDCD10 expression level in tumors larger than 3 cm was higher than in tumors smaller than 3 cm (Fig. 3G). Moreover, the PDCD10 expression level in stage III/IV tumors was higher than that in stage I/II tumors (Fig. 3H). miR-103 expression was negatively correlated with PDCD10 expression (Fig. 3I).

Downregulation of PDCD10 Is Involved in miR-103-Induced Inhibition of Proliferation and Migration of the A549 Cell Line

To test whether downregulation of PDCD10 is involved in miR-103-induced inhibition of proliferation and migration, A549 cells were cotransfected with the miR-103 mimic and PDCD10 plasmid. We showed that overexpression of PDCD10 significantly increased cell proliferation and suppressed miR-103 mimic-induced reduction of cell proliferation in A549 cells (Fig. 4A). Overexpression of PDCD10 notably decreased apoptotic cell death and suppressed miR-103 mimic-induced increase in apoptosis in A549 cells (Fig. 4B and C). Overexpression of PDCD10 notably decreased Bax expression and increased Bcl-2 expression in A549 cells (Fig. 4D and E). Moreover, overexpression of PDCD10 notably inhibited miR-103 mimic-induced increase in Bax expression and decrease in Bcl-2 expression (Fig. 4D and E). Furthermore, overexpression of PDCD10 remarkably suppressed miR-103 mimic-induced decrease in invasion (Fig. 4F) and migration (Fig. 4G) abilities and reduction of N-cadherin (Fig. 4H) and vimentin (Fig. 4I) expression.

miR-103 Overexpression Inhibits NSCLC Growth In Vivo and Promotes Mouse Survival

In the next step, we investigated the effects of miR-103 on transplanted tumor growth in vivo. In order to make tumor growth easier to monitor, the subcutaneous xenograft tumor model in nude mice was established to assess the tumor formation ability of A549/miR-NC and A549/miR-103 cells. At the end of the experiment, the subcutaneous xenograft tumors were excised and weighed. As shown in Figure 5A and B, tumor weight and volume in the miR-103 group were significantly larger than in the miR-NC group. Survival analysis revealed that the median overall survival was longer in mice transplanted with A549/miR-103 cells (Fig. 5C). qRT-PCR and Western blot

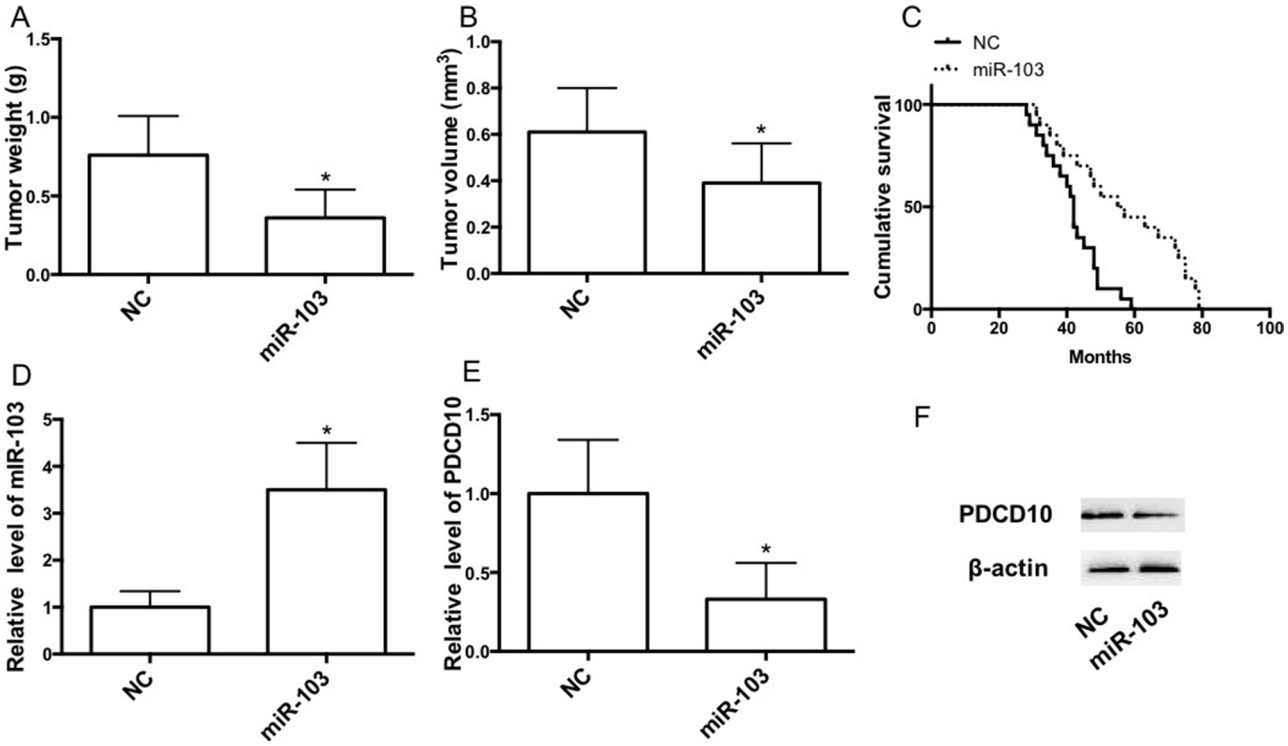

Figure 5. miR-103 suppresses the growth of NSCLC subcutaneous tumor. (A) Tumor weight. (B) Tumor volume. (C) Kaplan–Meier analyses of cumulative survival for mice with NSCLC subcutaneous tumor according to the expression of miR-103. (D–F) mRNA expression of miR-103 (D) and PDCD10 (E) and protein expression of PDCD10 (F) were determined by qRT-PCR and Western blot, respectively. Error bars represent the mean ± SEM. $*p < 0.05$, compared with control.

results showed that miR-103 expression in tumors was increased and that PDCD10 expression in tumors was decreased in the miR-103 group (Fig. 5D–F).

DISCUSSION

Accumulating evidence suggests that dysregulation of miRNAs plays a role in NSCLC development and is associated with histological subtypes, tumor stages, recurrent tumors, and overall survival[18,19]. It has been reported that miR-103 plays both positive and negative roles in different types of cancers. In colorectal cancer, miR-103 functioned as an oncogene via inhibition of tumor suppressors DICER and PTEN[14]. In gastric cancer, miR-103 promotes proliferation and metastasis via regulation of KLF4[20]. In hemopoietic tumor, miR-103 functioned as a tumor suppressor and sensitized cells for glucocorticoid-induced apoptosis[15]. In particular, miR-103 was recently identified to be negatively associated with metastatic capacity in primary lung tumors[17].

In the current study, we investigated the role of miR-103 in the development of NSCLC. We showed that miR-103 expression was reduced in NSCLC tissues and cells. miR-103 expression was negatively correlated with tumor size and stage. Kaplan–Meier analysis revealed that the median overall survival was longer in patients with higher miR-103 level than in those with lower miR-103 expression. The data demonstrated that miR-103 was a negative regulator for NSCLC. Moreover, we provided direct evidence for the negative role of miR-103 in NSCLC growth, indicating that miR-103 inhibited cell proliferation in A549 cells, decreased tumor weight and volume, and prolonged survival of tumor-implanted nude mice. miR-103 increased apoptotic cell death in A549 cells. Furthermore, miR-103 decreased the invasion and migration abilities in A549 cells, as evidenced by the Transwell and wound healing results.

Previous results have found several target genes of miR-103. For example, DICER and PTEN are the target genes in miR-103-induced promotion of colorectal cancer[14]. In human gastric carcinoma, miR-103 was found to modulate multidrug resistance by downregulation of Cav-1[21]. Zheng et al. showed that miR-103 promoted tumor growth and metastasis in colorectal cancer by directly targeting LATS2[22]. In prostate cancer, miR-103 suppressed tumor cell proliferation by targeting PDCD10[23]. PDCD10 is identified as an apoptosis-related gene that plays an important role in regulating cell apoptosis[24]. Overexpression of PDCD10 suppressed natural cell death in fibroblast cell lines exposed to specific apoptotic stimuli, such as staurosporine, cycloheximide, or tumor necrosis factor-α[25,26], suggesting an antiapoptotic role of PDCD10. However, the role of PDCD10 in NSCLC is not known. In the current study, we found that PDCD10 may be the target gene responsible for the tumor-suppressive role of miR-103 in NSCLC. Downregulation of miR-103 significantly reduced PDCD10 level. We found a significant decrease in the relative luciferase activity of the reporter gene in A549 cells cotransfected with the miR-103 mimic and pGL3-PDCD10 WT 3′-UTR, but not in pGL3-PDCD10 mut 3′-UTR. We showed that overexpression of PDCD10 significantly inhibited miR-103-induced inhibition of cell proliferation, increased apoptosis, and decreased invasion and migration in A549 cells. Moreover, we found that PDCD10 expression was increased in NSCLC tissues and cells. PDCD10 expression was positively correlated with tumor size and stage. Overexpression of PDCD10 increased cell proliferation and inhibited apoptosis in A549 cells. These results suggested that downregulation of PDCD10 mediated the inhibitory effect of miR-103 on NSCLC.

In summary, we identified that miR-103 functioned as a tumor suppressor in NSCLC, and PDCD10 is the direct target of miR-103 in the regulation of NSCLC cell proliferation and metastasis. Dysregulation of miR-103/PDCD10 signaling may be a novel therapeutic target for the treatment of NSCLC.

ACKNOWLEDGMENT: The authors declare no conflicts of interest.

REFERENCES

1. Chen W, Zheng R, Zuo T, Zeng H, Zhang S, He J. National cancer incidence and mortality in China, 2012. Chin J Cancer Res. 2016;28(1):1–11.
2. Chen W, Zheng R, Baade PD, Zhang S, Zeng H, Bray F, Jemal A, Yu XQ, He J. Cancer statistics in China, 2015. CA Cancer J Clin. 2016;66(2):115–32.
3. Ma L, Xie XW, Wang HY, Ma LY, Wen ZG. Clinical evaluation of tumor markers for diagnosis in patients with non-small cell lung cancer in China. Asian Pac J Cancer Prev. 2015;16(12):4891–4.
4. Walker S. Updates in non-small cell lung cancer. Clin J Oncol Nurs. 2008;12(4):587–96.
5. Osarogiagbon RU, Lin CC, Smeltzer MP, Jemal A. Prevalence, prognostic implications, and survival modulators of incompletely resected non-small cell lung cancer in the U.S. National Cancer Data Base. J Thorac Oncol. 2016;11(1):e5–16.
6. Wei R, DeVilbiss FT, Liu W. Genetic polymorphism, telomere biology and non-small lung cancer risk. J Genet Genomics 2015;42(10):549–61.
7. Chen Z, Fillmore CM, Hammerman PS, Kim CF, Wong KK. Non-small-cell lung cancers: A heterogeneous set of diseases. Nat Rev Cancer 2014;14(8):535–46.
8. Volinia S, Galasso M, Costinean S, Tagliavini L, Gamberoni G, Drusco A, Marchesini J, Mascellani N, Sana ME, Abu Jarour R, Desponts C, Teitell M, Baffa R, Aqeilan R, Iorio MV, Taccioli C, Garzon R, Di Leva G, Fabbri M, Catozzi M, Previati M, Ambs S, Palumbo T, Garofalo M, Veronese A, Bottoni A, Gasparini P, Harris CC, Visone R, Pekarsky Y, de la Chapelle A, Bloomston M, Dillhoff M, Rassenti LZ, Kipps TJ, Huebner K, Pichiorri F, Lenze D, Cairo S,

Buendia MA, Pineau P, Dejean A, Zanesi N, Rossi S, Calin GA, Liu CG, Palatini J, Negrini M, Vecchione A, Rosenberg A, Croce CM. Reprogramming of miRNA networks in cancer and leukemia. Genome Res. 2010;20(5):589–99.
9. Ambros V. The functions of animal microRNAs. Nature 2004;431(7006):350–5.
10. Zhang R, Su B. Small but influential: The role of microRNAs on gene regulatory network and 3′UTR evolution. J Genet Genomics 2009;36(1):1–6.
11. Cortinovis D, Monica V, Pietrantonio F, Ceresoli GL, La Spina CM, Wannesson L. MicroRNAs in non-small cell lung cancer: Current status and future therapeutic promises. Curr Pharm Des. 2014;20(24):3982–90.
12. Luo W, Huang B, Li Z, Li H, Sun L, Zhang Q, Qiu X, Wang E. MicroRNA-449a is downregulated in non-small cell lung cancer and inhibits migration and invasion by targeting c-Met. PLoS One 2013;8(5):e64759.
13. Keller A, Backes C, Leidinger P, Kefer N, Boisguerin V, Barbacioru C, Vogel B, Matzas M, Huwer H, Katus HA, Stähler C, Meder B, Meese E. Next-generation sequencing identifies novel microRNAs in peripheral blood of lung cancer patients. Mol Biosyst. 2011;7(12):3187–99.
14. Geng L, Sun B, Gao B, Wang Z, Quan C, Wei F, Fang XD. MicroRNA-103 promotes colorectal cancer by targeting tumor suppressor DICER and PTEN. Int J Mol Sci. 2014;15(5):8458–72.
15. Kfir-Erenfeld S, Haggiag N, Biton M, Stepensky P, Assayag-Asherie N, Yefenof E. miR-103 inhibits proliferation and sensitizes hemopoietic tumor cells for glucocorticoid-induced apoptosis. Oncotarget 2017;8(1):472–89.
16. Xiong B, Lei X, Zhang L, Fu J. miR-103 regulates triple negative breast cancer cells migration and invasion through targeting olfactomedin 4. Biomed Pharmacother. 2017;89:1401–8.
17. Garofalo M, Romano G, Di Leva G, Nuovo G, Jeon YJ, Ngankeu A, Sun J, Lovat F, Alder H, Condorelli G, Engelman JA, Ono M, Rho JK, Cascione L, Volinia S, Nephew KP, Croce CM. EGFR and MET receptor tyrosine kinase-altered microRNA expression induces tumorigenesis and gefitinib resistance in lung cancers. Nat Med. 2011;18(1):74–82.
18. Ma Y, Feng J, Xing X, Zhou B, Li S, Zhang W, Jiang J, Zhang J, Qiao Z, Sun L, Ma Z, Kong R. miR-1908 overexpression inhibits proliferation, changing Akt activity and p53 expression in hypoxic NSCLC cells. Oncol Res. 2016;24(1):9–15.
19. Huang J, Sun C, Wang S, He Q, Li D. microRNA miR-10b inhibition reduces cell proliferation and promotes apoptosis in non-small cell lung cancer (NSCLC) cells. Mol Biosyst. 2015;11(7):2051–9.
20. Zheng J, Liu Y, Qiao Y, Zhang L, Lu S. miR-103 promotes proliferation and metastasis by targeting KLF4 in gastric cancer. Int J Mol Sci. 2017;18(5).
21. Zhang Y, Qu X, Li C, Fan Y, Che X, Wang X, Cai Y, Hu X, Liu Y. miR-103/107 modulates multidrug resistance in human gastric carcinoma by downregulating Cav-1. Tumour Biol. 2015;36(4):2277–85.
22. Zheng YB, Xiao K, Xiao GC, Tong SL, Ding Y, Wang QS, Li SB, Hao ZN. MicroRNA-103 promotes tumor growth and metastasis in colorectal cancer by directly targeting LATS2. Oncol Lett. 2016;12(3):2194–2200.
23. Fu X, Zhang W, Su Y, Lu L, Wang D, Wang H. MicroRNA-103 suppresses tumor cell proliferation by targeting PDCD10 in prostate cancer. Prostate 2016;76(6):543–51.
24. Wang Y, Liu H, Zhang Y, Ma D. cDNA cloning and expression of an apoptosis-related gene, humanTFAR15 gene. Sci China C Life Sci. 1999;42(3):323–9.
25. Ma X, Zhao H, Shan J, Long F, Chen Y, Chen Y, Zhang Y, Han X, Ma D. PDCD10 interacts with Ste20-related kinase MST4 to promote cell growth and transformation via modulation of the ERK pathway. Mol Biol Cell 2007;18(6):1965–78.
26. Lu L, Ying K, Wei S, Liu Y, Lin H, Mao Y. Dermal fibroblast-associated gene induction by asiaticoside shown in vitro by DNA microarray analysis. Br J Dermatol. 2004;151(3):571–8.